NUMERICAL SIMULATION OF RUNOFF GENERATION AND INUNDATION PROCESS OF AN EXTREME PRECIPITATION EVENT IN NEPAL

ROCKY TALCHABHADEL
Disaster Prevention Research Institute, Kyoto University, Japan, rocky.ioe@gmail.com

HAJIME NAKAGAWA
Disaster Prevention Research Institute, Kyoto University, Japan, nakagawa@uh31.dpri.kyoto-u.ac.jp

KENJI KAWAIKE
Disaster Prevention Research Institute, Kyoto University, Japan, kawaike.kenji.5n@kyoto-u.ac.jp

KAZUKI YAMANOI
Disaster Prevention Research Institute, Kyoto University, Japan, yamanoi.kazuki.6s@kyoto-u.ac.jp

HERMAN MUSUMARI
Graduate School of Civil and Earth Resources Engineering, Kyoto University, Japan, hermusumari@gmail.com

TIRTHA R. ADHIKARI
Central Department of Hydrology and Meteorology, Tribhuvan University, Nepal, tirtha43@gmail.com

RAJARAM PRAJAPATI
Smartphones For Water Nepal, Nepal, rajaram@smartphones4water.org

ABSTRACT

Number of occurrences of heavy precipitation events is increasing rapidly in Nepal affecting lives and properties each year, especially in monsoon season (Jun-Sep). We investigated an extreme (heavy) precipitation and subsequent flooding event of Aug 2014 over the West Rapti River (WRR) basin, Nepal. We firstly used ground-based hourly rainfall data (9 stations) and a kinematic wave flow model was validated against ground-based hourly water level at an outlet of WRR basin. A shallow-water inundation model was then used to simulate the inundation process. Our results show similar spatial patterns of inundation with those derived from satellite images. This study also attempts to analyze the effectiveness of satellite-based rainfall estimates (SREs) in capturing extreme precipitation events. We used half-hourly data of IMERG (Early, Late and Final versions), resolution (10 km), and hourly data of 1) PERSIANN, resolution (25 km), and 2) PERSIANN-CCS, resolution (4 km). Similarly, we used 3-hour data of TMPA product real-time (3B42RT), resolution (25 km). In general, SREs represent the pattern of extreme precipitation in the study area but lack the precise representation on a sub-daily scale. This study assesses different corrections of SREs with respect to (wrt) ground-based data and fills data gaps of ground-based rainfall wrt SREs. There exists a great challenge into local flood simulation employing SREs.

Keywords: Extreme precipitation, Inundation, Satellite-based rainfall estimate, West Rapti River basin

1. INTRODUCTION

Heavy to very heavy precipitation (hereinafter extreme precipitation) events recurrently occur during monsoon season in Nepal (Karki et al. 2018; Talchabhadel et al. 2018). An extreme precipitation event of August 2014 is one of the seriously destructive events of recent time. Around the WRR basin, 24 h accumulated (08:45 Local Time i.e. 03UTC 14 Aug – 15 Aug 2014) precipitation of 528 mm was recorded at Chisapani station (location shown in Figure 1a), which is the highest ever recorded 24 h accumulated precipitation in Nepal. The torrential rain affected seriously and water levels in most of the rivers increased above warning and danger levels. In Babai River, adjacent to the WRR basin shown in Figure 1a, the early warning system (EWS) was completely washed away by the flood and no EWS worked which caused in human deaths in addition to huge property loss (Reliefweb 2014). Such a scenario highlights the importance of SREs at the time of failure of ground-based (hereinafter gauge) data. The rain gradually reduced from an afternoon of 15 August 2014 even though floodwaters took some days to recede from inundated villages. For a numerical analysis of such processes, sub-daily (e.g. hourly hydro-meteorological) data are required. The WRR basin has 4 discharge and 9 precipitation stations (shown in Figures 1c, and d) with sub-daily temporal resolution. We selected WRR basin for our analysis because other adjacent basins (i.e. Babai, Karnali) do not have sufficient sub-daily data.

This study applied a kinematic wave flow model on hill slopes for simulating surface runoff. A shallow-water unsteady flow model was used to simulate the inundation process. Firstly, the hydrological model was validated against gauge hourly discharge. The simulated surface runoffs from other hill slopes were then provided for an inundation analysis. We compared spatial patterns of inundation with those derived from satellite images. This study also attempts to analyze the effectiveness of SREs in capturing extreme precipitation events. This study used IMERG (Early, Late and Final versions), PERSIANN, PERSIANN-CCS, and TMPA products. In this study, we proposed different corrections of SREs wrt gauge data and at the same time, we also filled some data gaps of gauge data wrt SREs.

2. STUDY AREA

The study area, a catchment area of 6368 km^2 up to Nepal-India border, has a diverse elevation range (shown in Figure 1 b) varying from 100 m to 3600 m above-sea-level (asl) within a small latitude extent of nearly 1°. The response time of extreme precipitation events is very quick due to the steep topography. The mean annual precipitation (MAP) is about 1500 mm and more than 80 % of it occurs during the monsoon season. Figure 1c shows a spatial distribution of MAP across the study area. River valleys are comparatively drier. Figure 1 d shows a spatial distribution of total precipitation of the selected time period (Aug 10 – 19, 2014). A localized nature of heavy precipitation, almost 45% of the MAP, is observed around the station 3. Stations 1-5 (from left) are located in the lower elevation (0-500 m asl) and stations 6-9 (from left) are located in the upper region of the study area. Effectiveness of SREs is compared at these stations in the subsequent section.

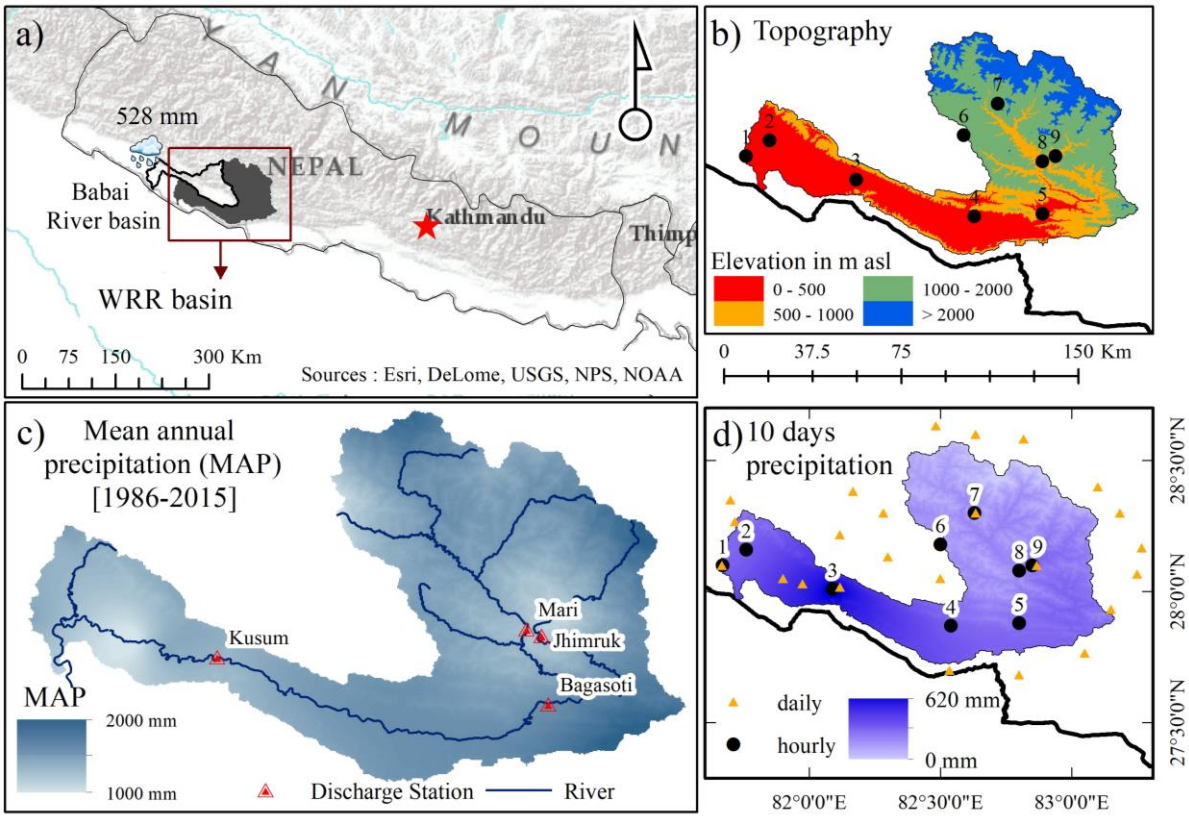

Figure 1. a) Locations of WRR basin, Babai River basin (adjacent to WRR basin), and Chisapani station (ever recorded 24 h accumulated precipitation) over Nepal, b) topography of the study area, c) spatial distribution of mean annual precipitation over the time period of 1986-2015 calculated using daily rainfall, and d) network of rainfall stations (daily and hourly) overlaid on spatial distribution of 10 days precipitation.

3. DATA AND METHODS

3.1 Hydro-meteorological data

We used hourly rainfall data of 9 automatic rainfall stations and water level data of 4 automatic hydrological stations distributed across the WRR basin maintained by the Department of Hydrology and Meteorology (DHM), Government of Nepal (GoN). Hourly discharge at stations was estimated employing the stage-discharge relation. The automatic network includes tipping bucket type precipitation gauges. Please see Talchabhadel et al. (2017) for the detailed information about precipitation measurement in Nepal. We used half-hourly data of IMERG (Early, Late and Final versions), resolution (10km), hourly data of PERSIANN, resolution (25 km), and PERSIANN-CCS, resolution (4 km), and 3-hour data of TMPA (3B42RT), resolution (25 km).

Integrated Multi-SatellitE Retrievals for GPM (IMERG) estimates rainfall from the various precipitation-relevant satellite passive microwave (PMW) sensors comprising Global Precipitation Measurement (GPM)

constellation are computed employing Goddard Profiling Algorithm (GPROF2017). Detailed information could be found in Huffman et al. (2019). We used a current version, i.e. 06B version, of Early, Late and Final products of IMERG. Early product is available after ~ 4 h of observation time, and Late product after ~14 h of observation time without concluding calibration whereas Final product is available after ~ 3.5 months of observation time after the concluding calibration based on monthly gauge analysis.

TRMM Multi-satellite Precipitation Analysis (TMPA) algorithm provides precipitation estimates in the Tropical Rainfall Measuring Mission (TRMM) regions that have the (nearly-zero) bias of the "TRMM Combined Instrument" precipitation estimate and the dense sampling of high-quality microwave data with fill-in using microwave-calibrated infrared estimates. We used a 3B42RT version7 TMPA product in this study. The TMPA products ended on December 31, 2019. New products to supersede the TMPA datasets are being produced under the GPM umbrella with the IMERG algorithm.

PERSIANN system developed by the Center for Hydrometeorology and Remote Sensing (CHRS) employs neural network function classification/approximation methods to estimate rainfall rate using the information of the infrared brightness temperature image provided by geostationary satellites. The system has an updating adaptive training feature of the parameters whenever independent estimates of rainfall are available. Model parameters are regularly updated using rainfall estimates from low-orbital satellites, including TRMM. PERSIANN-CCS is a real-time global high-resolution satellite product that enables the categorization of cloud-patch features based on cloud height, areal extent, and variability of texture estimated from satellite imagery. Precipitation intensity and distribution of classified cloud patches are initially trained using ground radar and TRMM observations. The PERSIANN-CCS enables recursive (in space and time) data assimilation and system training, allowing for flexibility in the adjustment of the cloud-rain distribution curves as new ground or space-based radar measurements become available.

Inter-comparisons of different data sources were conducted with gauged data at 9 station locations. At first, the gauge data was checked for any data gaps. At station locations without any data gaps, rainfall detection abilities of different SREs were evaluated using 4 statistical indices, namely 1) probability of detection (POD), 2) critical success index (CSI), 3) false alarm ratio (FAR), and 4) frequency bias index (FBI). Table 1 shows a detail of calculation of indices. POD denotes the proportion of the number of correctly detected rainfall events of SRE wrt to the number of rainfall occurrences observed by gauge data. Similarly, CSI displays an overall ratio of rainfall events correctly identified by SRE whereas FAR indicates the proportion of false status. POD, CSI and FAR vary from 0 to 1: with 0 being an ideal FAR and 1 being an ideal POD and CSI, and. FBI represents a simple bias between gauge data and SRE. Detection indices were calculated on hourly, 3-h, 6-h, 12-h, 18-h and 24-h scale.

Table 1. Statistical indices for rainfall detection evaluation

Status		Satellite	Gauge
True	T	Rainy	Rainy
False	F	Rainy	Non-Rainy
Miss	M	Non-Rainy	Rainy
Null	X	Non-Rainy	Non-Rainy

Detection indices		Equation	Range	Ideal Value
Probability of Detection	POD	T/(T+M)	0 to 1	1
Critical Success Index	CSI	T/(T+M+F)	0 to 1	1
False Alarm Ratio	FAR	F/(T+F)	0 to 1	0
Frequency Bias Index	FBI	(T+F)/(T+M)	0 to ∞	1

Rain threshold = 0.2 mm

For a magnitude-based evaluation of SREs, mean difference (MD), mean absolute difference (MAD), root mean square error (RMSE) and percentage bias (PBIAS) wrt gauge data were computed. Negative values of MD and PBIAS represent underestimation and positive values represent overestimation of SRE wrt gauge data. A lower value is ideal for all four magnitude-based indices. This study applied a simple linear scaling correction to SREs on an event basis at station locations with no data gaps. The gauge stations with data gaps were attempted to fill using the SREs having good performances.

3.2 Numerical simulation

An RRI model (Sayama 2012), developed by the International Center for Water Hazard and Risk Management (ICHARM), was used employing a kinematic wave model for hillslope and a river-routing model for river channel for simulating rainfall runoff processes in conjunction with a 2D shallow-water equation model (Hashimoto 2018) for inundation propagation A leap-frog difference scheme was employed to solve these equations. We used unstructured meshes (Kawaike 2000), i.e. triangular in shape for the computation. Smaller meshes were specified in the river system and relatively coarser meshes were specified for the remaining. The total number of computation meshes is 34670 with 18296 nodes. Manning's roughness coefficient for a river channel was given 0.025 and 0.04 was given for the remaining meshes. This study used 30 m spatial resolution Advanced World 3D (AW3D) and local information of 30 river cross-sections for a topographical input.

We firstly calibrated the hydrological model on the flood event of August 2012, one of the big floods in WRR during the recent time after the implementation of the automatic hydro-meteorological station. The WRR crossed the danger level for 19 h during that event (Talchabhadel and Sharma 2014). After checking the model applicability, it was applied for the case of August 2014. The hydrological model was fed with 1) gauge data, 2) SREs data, 3) bias-corrected SREs, and 4) gauge data after filling data gaps. Results obtained from the hydrological model were fed into the inundation model for simulating the inundation propagation downstream. We attempted to compare the spatial extent with satellite imagery. We believe the information from the developed model could be used for flood early warning in the coming days.

4. RESULTS AND DISCUSSIONS

4.1 Evaluation of SREs

Figure 2 shows basin averaged rainfall of the study area during the selected time period (Aug 10 – 19 2014) based on gauged data and different selected SREs. In general, PERSIANN and PERSIANN-CCS show an underestimation whereas IMERG (Early, Late and Final versions) and TMPA show an overestimation wrt to gauge data on a spatially average scale. Clear information of heavy precipitation from the evening of 14 August to the afternoon of 15 August is depicted by all products. However, SREs show an occurrence of rainfall on the morning of 14 August which is not shown by the gauge data. Detection and magnitude-based indices are used for evaluation of performance of SREs.

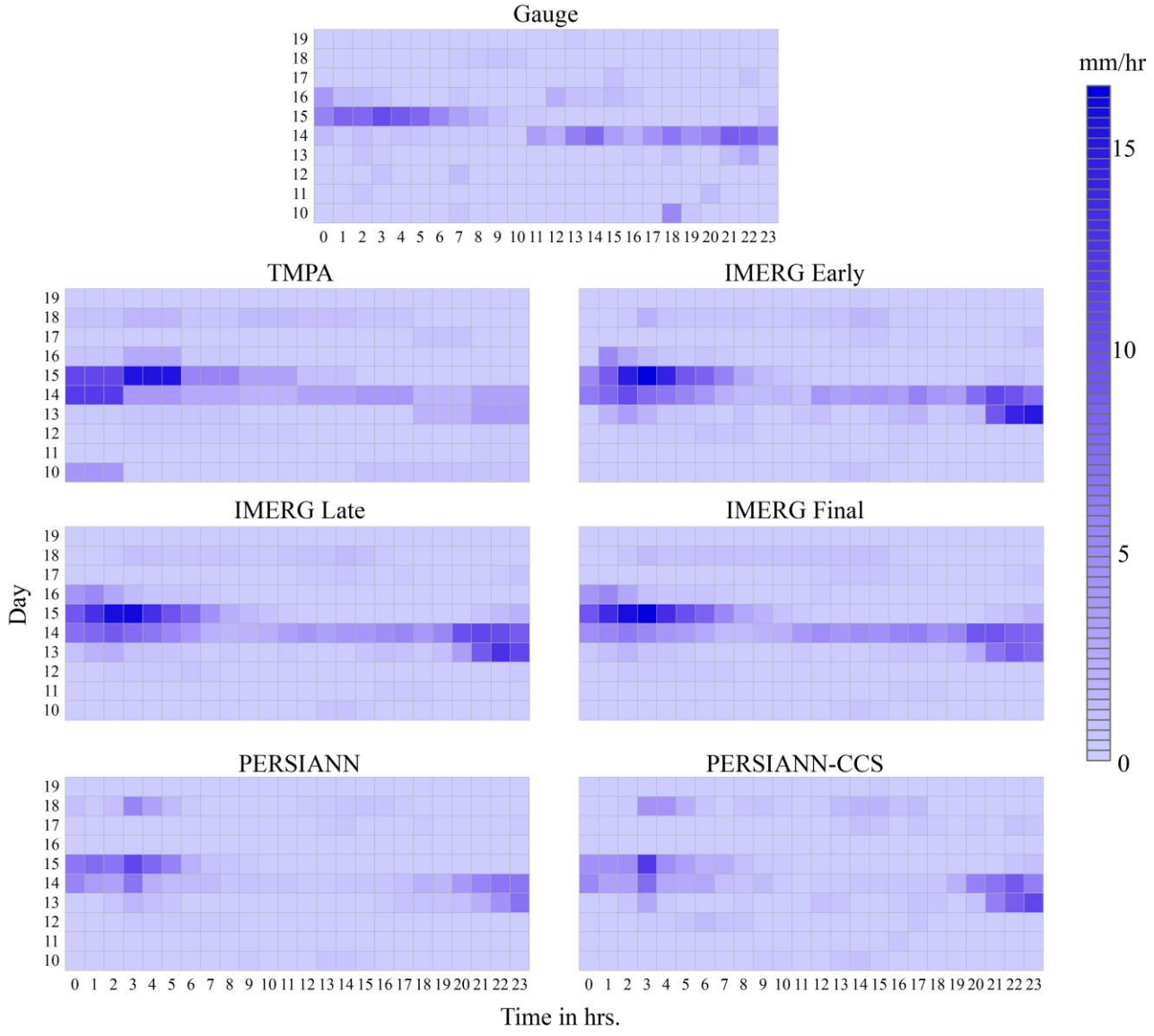

Figure 2 Basin averaged rainfall of the study area during Aug 10 – 19, 2014 based on gauged data and different SREs.

At first, we need to understand the reliability of the gauge data. For instance, station 2 did not record any rainfall throughout the study time period. Similarly, stations 1 and 9 have data gaps more than 35% of the time and station 4 has data gaps almost 60% of the time. The remaining 5 stations have uninterrupted data during selected time period. Detection and magnitude-based indices were calculated at these 5 station locations for the evaluation of the performance of SREs. Table 2 shows a summary of total rainfall during the selected time

period at station locations based on gauge data and different SREs. A linear correction factor (CF) on a 10 days event scale was computed at station locations for the stations without any data interruption. Out of 5 stations, 4 stations show underestimation for PERSIANN and PERSIANN-CCS. Other SREs show overestimation most of the time except for station 3 for IMERG-Final and TMPA. There exist two main challenges in the use of such data: 1) filling the gauge data gap and 2) correcting SREs.

Table 2. Correction factors for SREs at station locations wrt to gauge data over the study area for the selected time period (Aug 10 – 19 2014).

	Station 1	Station 2	Station 3	Station 4	Station 5	Station 6	Station 7	Station 8	Station 9
Gauge	52.40	0.00	620.00	11.80	278.60	112.40	182.60	189.20	13.60
No data hours	82	241	0	141	0	0	0	0	91
PERSIANN	206.83	206.83	181.87	171.01	150.07	154.41	126.55	150.07	150.07
CF_PERSIANN	1.00	1.00	**3.41**	1.00	**1.86**	0.73	**1.44**	**1.26**	1.00
PERSIANN-CCS	334.00	298.00	288.00	215.00	160.00	135.00	102.00	157.00	119.00
CF_PERSIANN-CCS	1.00	1.00	**2.15**	1.00	**1.74**	0.83	**1.79**	**1.21**	1.00
IMERG-E	421.75	469.51	653.01	324.85	340.12	308.73	193.32	214.83	224.55
CF_IMERG-E	1.00	1.00	0.95	1.00	0.82	0.36	0.94	0.88	1.00
IMERG-L	422.38	501.62	699.20	339.31	381.57	319.97	198.04	207.81	227.88
CF_IMERG-L	1.00	1.00	0.89	1.00	0.73	0.35	0.92	0.91	1.00
IMERG-F	293.57	317	354.49	314.72	362.92	276.78	287.09	260.35	308.09
CF_IMERG-F	1.00	1.00	**1.75**	1.00	0.77	0.41	0.64	0.73	1.00
TMPA	327.63	351.45	295.14	316.59	338.97	277.38	256.92	303.93	303.93
CF-TMPA	1.00	1.00	**2.10**	1.00	0.82	0.41	0.71	0.62	1.00

CF : Correction Factor

Bold values represent understimation of SREs

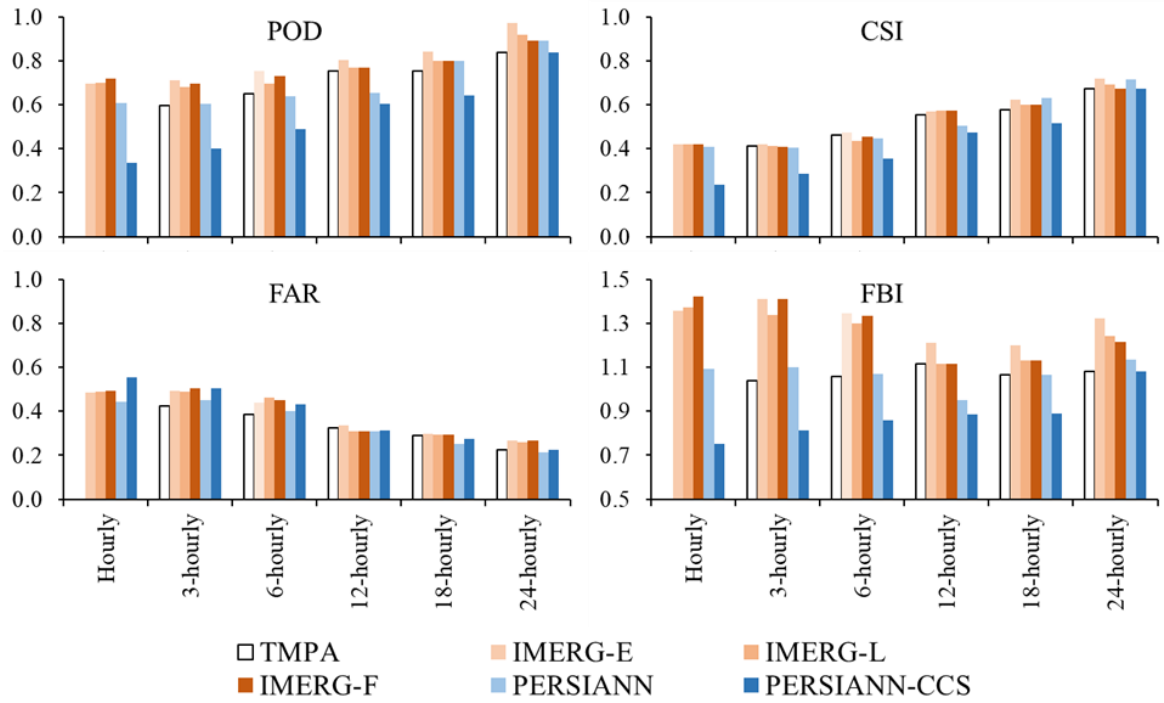

Figure 3 Performance of different SREs wrt gauge data on different time scales (hourly, 3h, 6h, 12h, 18h, and 24h) in the study area during Aug 10 – 19, 2014

Figure 3 shows the performance of different SREs on different hourly, 3-h, 6-h, 12-h, 18-h and 24-h scale. Rainfall detection indices on a coarser temporal resolution are showing better values (i.e. towards ideal value shown in Table 1), indicating the fact that SREs are performing quite well on a daily scale. In general, all SREs have a noteworthy false alarm and FAR values are almost similar to each other. On an hourly scale, FAR values are around 0.5 and on a daily scale they are around 0.25. PERSIANN seems to be better in terms of FAR and FBI, however, PERSIANN is inferior to IMERG (Early, Late and Final versions) in terms of POD. PERSIANN-CCS is the most poor-performed SRE. Table 3 shows values of error of different SREs wrt to the gauge data on an hourly scale. PERSIANN and PERSIANN-CCS are highly underestimating rainfall indicating a requirement of bias-correction. IMERG Early and IMERG Late have relatively higher positive biases. IMERG Final version

is significantly improved from Early and Late versions. TMPA has the lowest mean deviation and PBIAS, however, RMSE and MAD values are larger indicating a mismatch between SRE and gauge data on an hourly scale.

Table 3. Error evaluation of different SREs wrt gauge data in the study area during Aug 10 – 19, 2014

Magnitude based indices	TMPA	IMERG-E	IMERG-L	IMERG-F	PERSIANN	PERSIANN-CCS
MD (mm/h)	0.07	0.27	0.35	0.13	-0.51	-0.43
MAD (mm/h)	1.38	1.58	1.61	1.32	1.10	1.39
RMSE (mm/h)	4.07	5.19	5.32	4.15	3.91	4.67
PBIAS (%)	6.48	23.66	30.65	11.49	-44.82	-37.52

Uniform hourly rain is used for TMPA 3 h resolution.

We conducted 7 cases of hydrological simulation using gauge data and 6 individual SREs. Since PERSIANN and PERSIANN-CCS underestimated rainfall significantly we corrected them using above mentioned CFs and simulated 2 more cases. For a gauge data filling, we used an additional 4 cases incorporating TMPA and IMERG (Early, Late and Final versions) at data gap time. Figure 4 Left shows a comparison plot between simulated and observed hourly discharge at three outlets (upstream, midstream and downstream) during calibration period of Aug 1 – 10, 2012. Though base flow is not precisely represented by the model, peaks are in an acceptable range. The calibrated roughness coefficients for slopes and river channels were 0.1 and 0.018 respectively. We are still trying to calibrate other parameters for better results. The developed model was then used for the study time period (Aug 10 – 19, 2014). Figure 4 Right shows the hydrological response of the extreme precipitation event of August 2014. Our result shows that the peak value could not be matched precisely but the tendency of the hydrograph is congruous. Since gauge data suffers data gaps in a few stations, interpolation from the limited stations may bring an underestimation. We tried to fill gauge data gaps with different SREs to evaluate this issue. In addition, tipping bucket type automatic rainfall measurement normally underestimates by about 10 % when compared with manual rain gauges (Talchabhadel et al. 2017). One of possible reasons for underestimation in simulated discharge may be due to underestimation of precipitation estimates by tipping bucket method. In case of WRR basin, out of 9 stations only 3 stations are collocated with automatic and manual rain gauges. Therefore, station wise comparisons were not straight forward possible.

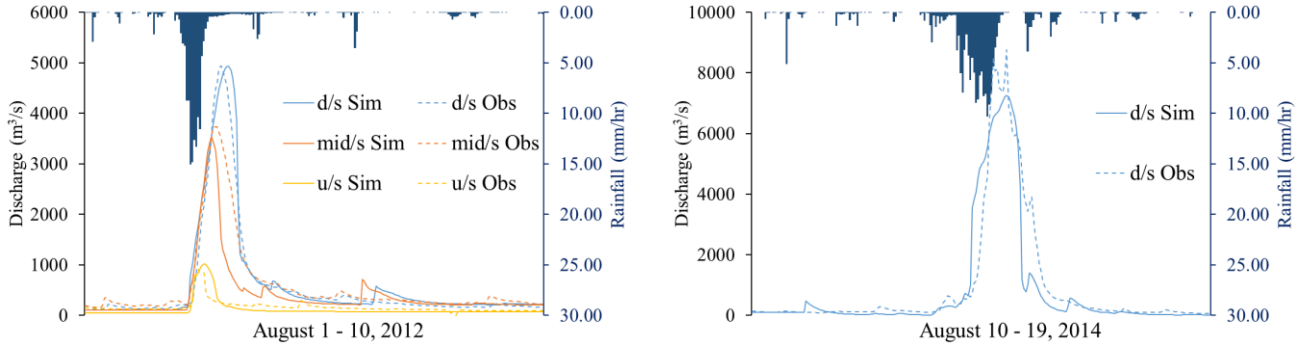

Figure 4 Comparisons of simulated and observed discharges at for the time period of Aug 1 – 10, 2012 [Left], and the study time period Aug 10 – 19 [right]. During the study time period the water level at u/s and mid/s stations were not recorded due to technical issues. Inverted bars represent basin averaged rainfall.

Figure 5 shows hydrological responses of the study area based on different data sources. Figure 5 a) shows comparison plot between observed, and simulated discharge from gauge, PERSIANN and PERSIANN-CCS. As mentioned earlier both PERSIANN and PERSIANN-CCS have underestimated rainfall as a result of which simulate discharges are also highly underestimated. After performing a bias correction, peak discharge is increased but still underestimated. Most importantly due to false alarm before a peak rain there is a double peak nature of hydrograph. It suggests to use a temporally dynamic bias correction on a sub-daily to daily scale rather than using a static CF based on an event. IMERG (Early, Late and Final) and TMPA show superior results than PERSIANN and PERSIANN-CCS. Double peak is still visible but it is found to be comparatively lesser in IMERG Final and TMPA. By looking into simulation results, IMERG Final proves to be better in terms of hydrograph nature even though it does have a slight overestimation. Similarly, looking at the magnitude of peak value, IMERG Late and TMPA perform better though they have significant false alarms prior to peak rainfall event. Number of automatic rainfall gauges should be increased, and these stations should be taken care for a proper continuity, and regular maintenance. In addition, introduction of x-radar is quite demanding for a precise understanding of dynamics of heavy precipitation events and numerical simulation of catchment response on such extreme precipitation.

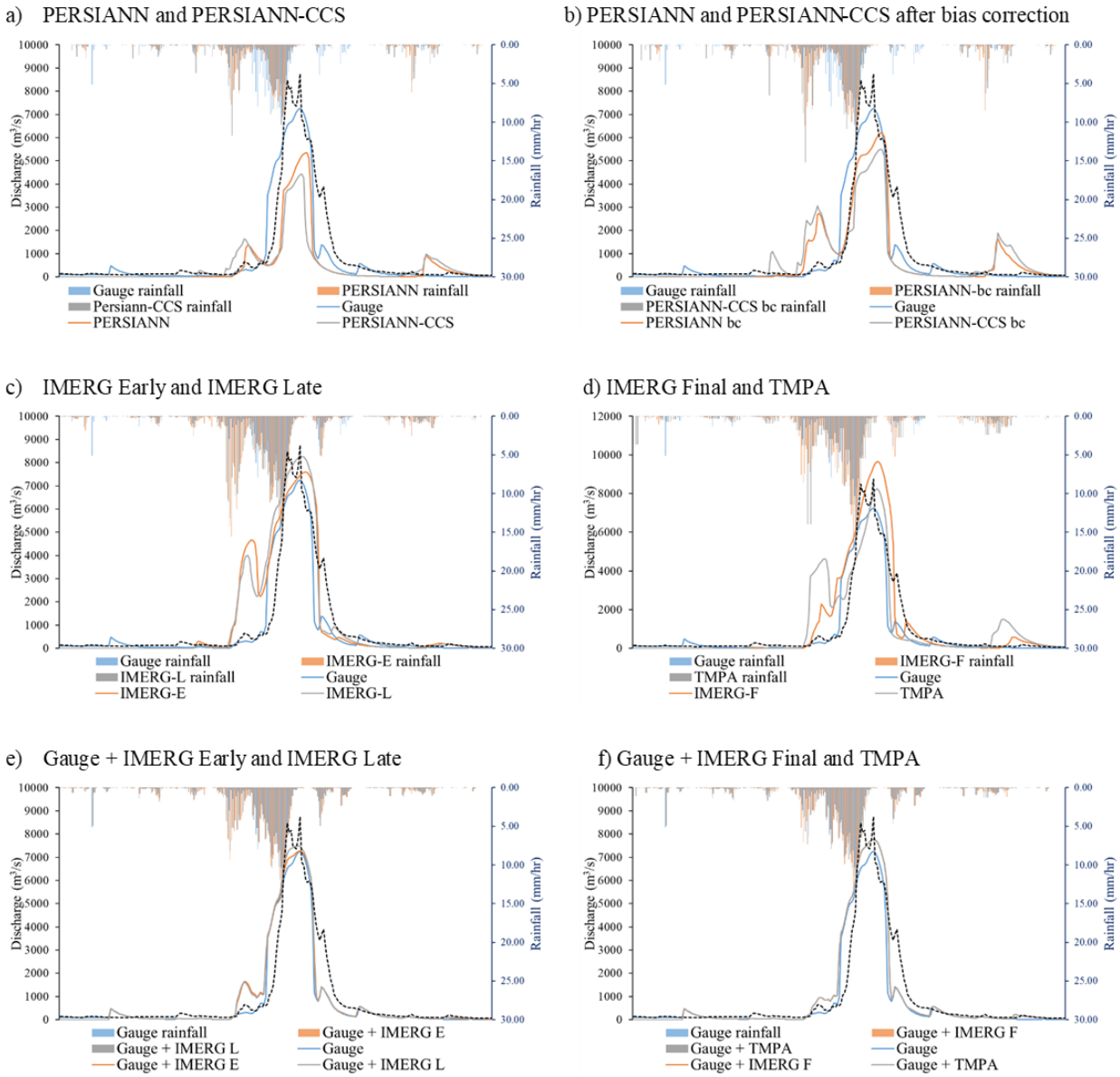

Figure 5 Comparisons of observed (black dotted) and simulated discharges (solid) based on gauge rainfall (blue) and different SREs in different cases: a) PERSIANN and PERSIANN-CCS, b) PERSIANN and PERSIANN-CCS after bias correction, c) IMERG Early and Late versions, d) IMERG Final and TMPA, e) Gauge data filled using IMERG Early and Late versions, and f) Gauge data filled using IMERG Final and TMPA. Basin averaged rainfall for different data sources are shown by inverter bars.

The inundation propagation model was fed with the simulated discharges of the hydrological model as an inflow boundary condition (locations shown in Figure 6 a). Figure 6 b) shows the numerically simulated inundation map for the case of Gauge + IMERG Final version (other cases not shown) and 6c) shows the extent of the frequently inundated map of the WRR basin. Most of the settlements prone to inundation are located near to Nepal-India border. The satellite-derived inundation map during other monsoon days (cloud cover for the same event is very high) also shows a similar extent of inundation. Generally, the anticipated impact of a disaster is estimated from the potential vulnerability of its critical facilities in a hazardous environment. We believe our results may provide supplementary information for the preparation of hazard maps in the study area. This study limits the quantitative comparisons of inundation depth with observed inundation. A perception-based analysis (questionnaire survey during a site visit in July 2019) supports the simulated results.

Overall, our results reveal the prospective of SREs' application for the numerical simulation of runoff and inundation scenario. At the complete wash away of the hydro-meteorological monitoring system (though not desired), SREs play a vital role in understanding the hydrological and hydrodynamic response of the catchment. In addition, SREs are also equally important to fill gauge data gaps. Based on the presented results, we recommend the use of IMERG products for the numerical simulation of extreme precipitation. However, this study is based on a single event and does not allow to draw a general conclusion. Therefore, further research is necessary in order to evaluate the performance of SREs. Gauge data are always valuable information. Thus proper maintenance and continuous operation are recommended.

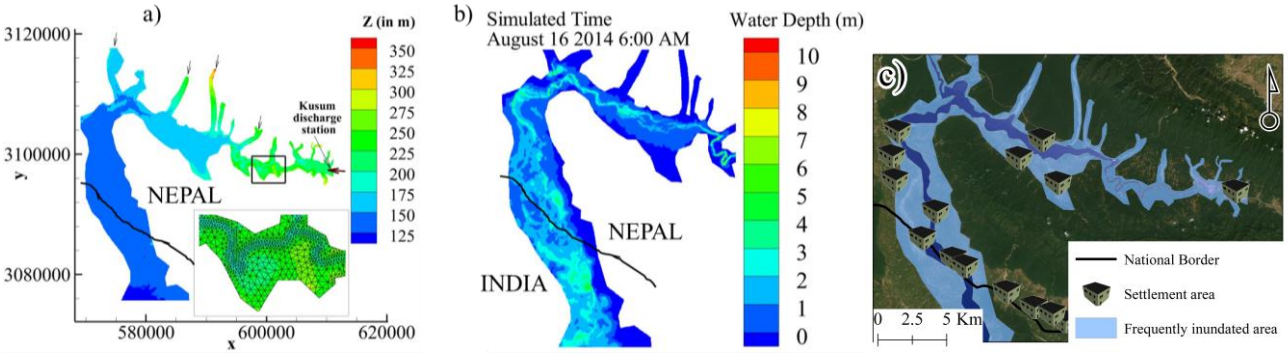

Figure 6 a) Topography of downstream of Kusum station for inundation modeling and a representative illustration of an unstructured computation mesh, and b) simulated inundation. Black arrows in figure a) indicate locations of simulated discharge input from different hill slopes for the case of Gauge + IMERG Final, and c) overlay of settlement and frequently inundated area..

5. CONCLUSIONS

Extreme precipitation induced disasters like floods, landslides, debris flow, and inundation are becoming more frequent. In this study, we investigated the extreme precipitation event of August 2014. This study used a kinematic wave flow model on hill slopes for simulating surface runoff and shallow-water model for inundation propagation. This study attempted to analyze the effectiveness of different SREs in capturing extreme precipitation events using different detection and magnitude-based indices. Overall, IMERG and TMPA have better performance than PERSIANN and PERSIANN-CCS. IMERG-Late version has superior results on numerical simulation. For PERSIANN and PERSIANN-CCS, we applied bias correction at the station locations and got fairly better results. At the same time, we also filled the gauge data gaps using different good-performed SREs and found more congruous results with observed discharge. False alarm values of all SREs are found to significantly high as a result of which numerical simulations show double peak features. For a precise replication of the rainfall scenario, the inclusion of bias correction of SREs should be done on a daily or sub-daily basis. At the same time, the performance of gauge data should also be checked properly by comparing it with other data sources. Our future works include the dynamic bias correction of SREs.

ACKNOWLEDGMENTS

This work was supported by the Japan Society for the Promotion of Science Postdoctoral Fellowship Program (grant in aid P19052). We would like to thank the Department of Hydrology and Meteorology for providing the observed rainfall and discharge data.

REFERENCES

Hashimoto, M., Yoneyama, N., Kawaike, K., Deguchi, T., Hossain, M.A., and Nakagawa, H. (2018). Flood and Substance Transportation Analysis Using Satellite Elevation Data: A Case Study in Dhaka City, Bangladesh. *Journal of Disaster Research*, 13(5).

Huffman, G. J., Bolvin, D. T., Braithwaite, D., Hsu, K-L, Joyce, R., Kidd, C., Nelkin, E. J., Sorooshian, S., Tan, J., and Xie, P. (2019). *Algorithm Theoretical Basis Document (ATBD) Version 06 NASA GPM IMERG*

Karki, R., Hasson, S. ul., Gerlitz, L., Talchabhadel, R., Schenk, E., Schickhoff, U., Scholten, T., and Böhner, J. (2018). WRF-based simulation of an extreme precipitation event over the Central Himalayas: Atmospheric mechanisms and their representation by microphysics parameterization schemes. *Atmospheric Research*, 214(February): 21–35.

Kawaike, K., Inoue, K. and Toda, K. (2000): Inundation modeling in urban area based on unstructured meshes. *Hydrosoft, Hydraulic engineering software*, 457-466.

Reliefweb. (2014). *Floods and Landslides DREF operation MDRNP007; Emergency Plan of Action (EPoA)*.

Sayama, T., Ozawa, G., Kawakami, T. and Nabesaka, S.(2012). Rainfall–Runoff–Inundation Analysis of the 2010 Pakistan Flood in the Kabul River Basin. *Hydrological Sciences Journal* **57**(2): 298–312.

Talchabhadel, R., Karki, R., and Parajuli, B. (2017). Intercomparison of precipitation measured between automatic and manual precipitation gauge in Nepal. *Measurement*, 106: 264–273.

Talchabhadel, R., Karki, R., Thapa, B. R., Maharjan, M., and Parajuli, B. (2018). Spatio-Temporal Variability of Extreme Precipitation in Nepal. *International Journal of Climatology* 38: 4296–4313. DOI: 10.1002/joc.5669.

Talchabhadel, R., and Sharma, R. (2014). Real Time Data Analysis of West Rapti River Basin of Nepal. *Journal of Geoscience and Environment Protection*, (December): 1–7.